AFOSR Project Report

Project Title: Complex-Shaped Microcomponents by the Reactive Conversion of Biological Templates

Award Number: FA9550-04-1-0022

Start Date: Dec. 15, 2003

Program Manager: Dr. Hugh C. De Long
Program Manager
Biomimetics, Biomaterials, and Biointerfacial Sciences
Air Force Office of Scientific Research
801 N. Randolph St., Room 732
Arlington, VA 22203-1977
E-mail: hugh.delong@afosr.af.mil
Phone: :(703) 696-7722
Fax: (703) 696-8449

Principal Investigator: Prof. Ken H. Sandhage
School of Materials Science & Engineering
Georgia Institute of Technology
771 Ferst Drive
Atlanta, GA 30332-0245
E-mail: ken.sandhage@mse.gatech.edu
Phone: (404) 894-6882
Fax: (404) 894-9140

Co-Investigators: Dr. Rajesh Naik, Group Leader
Biotechnology Group, MLPJ Hardened Materials Branch
Air Force Research Laboratory, Wright-Patterson AFB
3005 P Street
WPAFB, OH 45433-7702
E-mail: rajesh.naik@wpafb.af.mil
Phone: (937) 255-3808 ext. 3180
Fax: (937) 255-1128

DISTRIBUTION STATEMENT A
Approved for Public Release
Distribution Unlimited

20050627 096

REPORT DOCUMENTATION PAGE

AFRL-SR-AR-TR-05-

0239

Public reporting burden for this collection of information is estimated to average 1 hour per response, including the time for reviewing instructions data needed, and completing and reviewing this collection of information. Send comments regarding this burden estimate or any other aspect of this burden to Department of Defense, Washington Headquarters Services, Directorate for Information Operations and Reports (0704-0188), 121 4302. Respondents should be aware that notwithstanding any other provision of law, no person shall be subject to any penalty for failing to comp valid OMB control number. **PLEASE DO NOT RETURN YOUR FORM TO THE ABOVE ADDRESS.**

1. REPORT DATE *(DD-MM-YYYY)*	2. REPORT TYPE	3. DATES COVERED *(From - To)*
20-06-2005	Final Performance Report	Dec. 2003 to Dec. 2004

4. TITLE AND SUBTITLE
Complex-Shaped Microcomponents by the Reactive Conversion of Biological Templates

5a. CONTRACT NUMBER

5b. GRANT NUMBER
FA9550-04-1-0022

5c. PROGRAM ELEMENT NUMBER

6. AUTHOR(S)
Sandhage, Kenneth H.

5d. PROJECT NUMBER

5e. TASK NUMBER

5f. WORK UNIT NUMBER

7. PERFORMING ORGANIZATION NAME(S) AND ADDRESS(ES)

Georgia Tech. Research Corporation
Georgia Institute of Technology
505 Tenth Street, NW
Atlanta, GA 30332-0420

8. PERFORMING ORGANIZATION REPORT NUMBER

9. SPONSORING / MONITORING AGENCY NAME(S) AND ADDRESS(ES)
Air Force Office of Scientific Research
4015 Wilson Blvd Room 713
Arlington, VA 22203-1954
Program Manager: Dr. Hugh De Long
(703) 696-7722, hugh.delong@afosr.af.mil

10. SPONSOR/MONITOR'S ACRONYM(S)
USAF, AFRL

11. SPONSOR/MONITOR'S REPORT NUMBER(S)

12. DISTRIBUTION / AVAILABILITY STATEMENT
Approve for Public Release: Distribution Unlimited

13. SUPPLEMENTARY NOTES

14. **ABSTRACT** This project has been aimed at: 1) developing a better understanding of the manner in which the morphology and nanostructure of biologically-derived silica microtemplates evolve during the course of reactive conversion, and 2) determining which reaction parameters have the greatest impact on changes in morphology during such reactive conversion. The most significant accomplishments have been:

- Demonstration (via high resolution TEM analyses) that the reaction of SiO_2 diatom frustules with Mg(g) at 650°C results in direct conversion into nanocrystalline MgO and Si (≤15 nm) without the formation of intermediate silicate phases.
- Syntheses of MgO-converted frustules with minimal secondary phases (Si or Mg_2Si) by development of an optimized thermal treatment and selective dissolution treatment.
- Identification and control of critical processing parameters to avoid active vaporization and gas-phase-assisted coarsening during the metathetic conversion of SiO_2 frustules into TiO_2.
- Successful syntheses of ZrO_2 frustule replicas via a new two-step reaction process (conversion of SiO_2 into MgO via Mg(g) reaction; then conversion of MgO into ZrO_2 via $ZrCl_4$(g) metathetic reaction and selective $MgCl_2$ dissolution in water).

15. SUBJECT TERMS

16. SECURITY CLASSIFICATION OF:			17. LIMITATION OF ABSTRACT	18. NUMBER OF PAGES	19a. NAME OF RESPONSIBLE PERSON
a. REPORT	b. ABSTRACT	c. THIS PAGE			19b. TELEPHONE NUMBER *(include area code)*

Objectives: 1) To develop a better understanding of the manner in which the morphology and nanostructure of biologically-derived silica microtemplates evolve during the course of reactive conversion, and 2) to determine which reaction parameters have the greatest impact on changes in morphology during such reactive conversion.

Summary of Effort: Work over the past year has focused on the conversion of silica-based diatom frustules by the net reactions:

$$2Mg(g) + SiO_2(s) \Rightarrow 2MgO(s) + \{Si\} \quad (1)$$

$$TiF_4(g) + SiO_2(s) \Rightarrow TiO_2(s) + SiF_4(g) \quad (2)$$

$$ZrCl_4(g) + 2MgO(s) \Rightarrow ZrO_2(s) + 2MgCl_2(l) \quad (3)$$

where {Si} refers to Si in a Mg-Si liquid. Conversion of SiO_2-based diatom frustules into MgO, TiO_2, and ZrO_2 has been achieved with a preservation of the starting biogenic shapes.

Complete conversion of diatom frustules into MgO via net reaction (1) has been achieved at temperatures as low as 650°C within 2 h. Under these conditions, polycrystalline MgO frustules were generated with crystallite sizes of only 10-15 nm (i.e., much finer that for conversion at 900°C). TEM analyses of partially-converted specimens revealed the presence of MgO and Si nanocrystals ($\leq$5 nm in dia.) in close proximity within an unreacted silica matrix; that is, the conversion of SiO_2 appears to proceed directly without the formation of intermediate silicate phases (as has been reported in the literature for the reaction of Mg(g) gas with bulk SiO_2 at 1150°C). The solid Si product then reacted with excess Mg(g) to form Mg_2Si. The amount of Mg_2Si generated by this latter reaction was minimized by controlling the Mg:SiO_2 reactant ratio and the reaction temperature and time. A sodium hydroxide solution was then used to selectively dissolve away the Si product of reaction (1) to yield MgO-based frustule replicas.

Complete conversion of SiO_2-based diatom frustules into TiO_2 via the net reaction (2) has been accomplished at only 350°C via a two-step process: i) the formation of $TiOF_2(s)$ via reaction with $TiF_4(g)$ and then ii) conversion of $TiOF_2(s)$ into $TiO_2(s)$ via reaction with $O_2(g)$. By controlling the TiF_4:SiO_2 reactant ratio, the heating rate, and the peak reaction temperature and time during the first stage of reaction, active vaporization (due to $TiOF_2(s)$ formation away from the frustule surface) and coarsening (via a gas phase diffusion mechanism) were minimized so as to yield $TiOF_2$ replicas that preserved the starting frustule shape and fine features.

A two-step reaction process has also been developed to allow for chemical conversion of the silica-based diatom frustules into zirconia. Initial attempts to form ZrO_2 replicas via direct reaction of $ZrF_4(g)$ with $SiO_2(s)$ resulted in disintegration of the frustules. To avoid the formation of volatile Si-O-bearing products associated with such disintegration, the SiO_2 frustules were first converted into MgO via net reaction (1). The MgO replicas were then exposed to $ZrCl_4(g)$ at 650°C for 2 h to allow for reaction (3). The latter reaction yielded tetragonal ZrO_2 replicas along with a liquid $MgCl_2$ product that then solidified during cooling. Selective dissolution of the solidified magnesium chloride in water then yielded free-standing zirconia frustule replicas.

The reaction-based processes developed in this BioInspired Concepts (BIC) project have enabled the syntheses of frustule-shaped structures that exhibit:

i) luminescence (from Eu/$BaTiO_3$ coatings applied to compatible MgO-converted frustules)

ii) gas sensing (due to rapid changes in the conductivity of TiO_2 frustules resulting from small changes in ethanol vapor pressure)

iii) organophosphor destruction (pesticide-bearing solutions have exhibited rapid reaction with TiO_2-converted frustules)

Accomplishments/New Findings:

- Demonstration (via high resolution TEM analyses) that the reaction of SiO_2 diatom frustules with Mg(g) at 650°C results in direct conversion into nanocrystalline MgO and Si (≤15 nm) without the formation of intermediate silicate phases.
- Syntheses of MgO-converted frustules with minimal secondary phases (Si or Mg_2Si) by development of an optimized thermal treatment and selective dissolution treatment.
- Identification and control of critical processing parameters to avoid active vaporization and gas-phase-assisted coarsening during the metathetic conversion of SiO_2 frustules into TiO_2.
- Successful syntheses of ZrO_2 frustule replicas via a new two-step reaction process (conversion of SiO_2 into MgO via Mg(g) reaction; then conversion of MgO into ZrO_2 via $ZrCl_4$(g) metathetic reaction and selective $MgCl_2$ dissolution in water).

These new accomplishments have made possible the development (in a MURI project) of luminescent diatom frustules (for microtagging applications), single diatom frustule gas sensors (for minimally-invasive sensing), and diatom frustules that rapidly destroy organophosphorous compounds (potentially for removing chemical warfare agents).

Reactive Conversion into MgO Frustules

Phase and Nanostructural Evolution at 650°C

In order to slow down the rate of reaction (to enable evaluation of the earliest stage(s) of the MgO conversion process) *Aulacoseira* diatom frustules were exposed to Mg(g) at only 650-700°C. The frustules were placed inside and near one end of a mild steel tube. Mg granules (99.8% purity, 0.3-1.7 mm size) were placed at the other end of the tube. An excess of Mg granules relative to silica frustules ($Mg:SiO_2$ molar ratio = 9.9:1) was placed inside the steel tubes in order to ensure that the source of magnesium vapor was not depleted during the course of the reaction. The tube was then crimped and welded shut within an Ar atmosphere inside a glove box. The resulting sealed steel ampoule was then bent into an inverted "V" shape, in order to ensure that the silica frustules remained physically separated from the magnesium powder. The sealed steel ampoules were then heated at 5-7°C/min to 650°C or 700°C and held for 0.5-2 h.

A secondary electron image of a starting *Aulacoseira* diatom frustule, and an associated energy-dispersive x-ray (EDX) pattern are shown in Figures 1a and 1b, respectively (note: the gold peak was obtained from a thin coating applied to avoid electron beam charging).

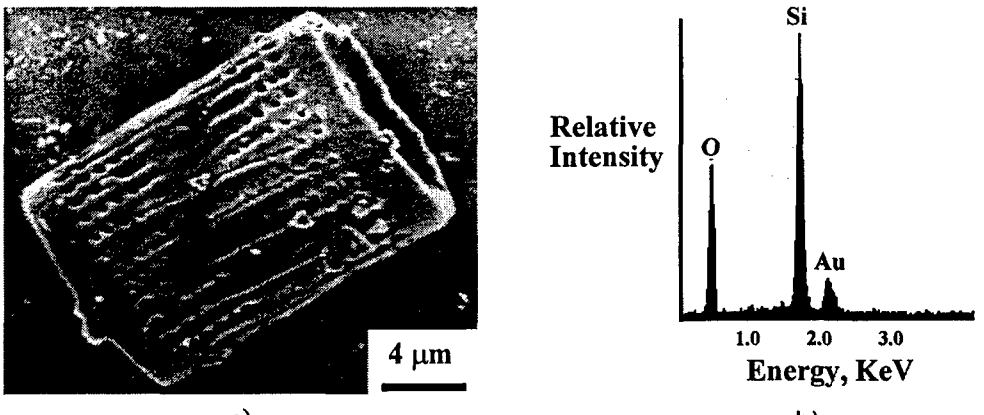

Fig. 1. a) Secondary electron image and b) EDX analysis of an *Aulacoseira* diatom frustule.

Upon heating to 650-700°C, the silica frustules within the sealed steel tube were exposed to magnesium gas generated by evaporation from the magnesium granules. Magnesium gas may undergo the following oxidation-reduction (displacement) reaction with silica:

$$2Mg(g) + SiO_2(s) \Rightarrow 2MgO(s) + Si(s) \qquad (4)$$

A secondary electron image of an *Aulacoseira* frustule that had been exposed to Mg(g) for 0.5 h at 700°C is shown in Fig. 2a. The cylindrical shape, narrow channels, and rows of fine pores were well preserved in this reacted frustule. A TEM image of a cross-section of such a reacted frustule is shown in Fig. 2b. The cross-section was comprised largely of crystallites with diameters ≤50 nm, although a few larger crystallites (100-150 nm diameter) were also detected. EDX (Fig. 2c) and electron diffraction (Fig. 2d) analyses revealed that the reacted frustule was comprised of magnesium oxide (periclase), with very little silicon detected throughout the cross-section (the gold peak in Fig. 2c was obtained from a coating applied to the specimen for SEM analysis prior to ion milling; the copper peak was obtained from the grid used to support the specimen cross-section in the TEM). The loss of silicon was a result of the formation of a Mg-Si

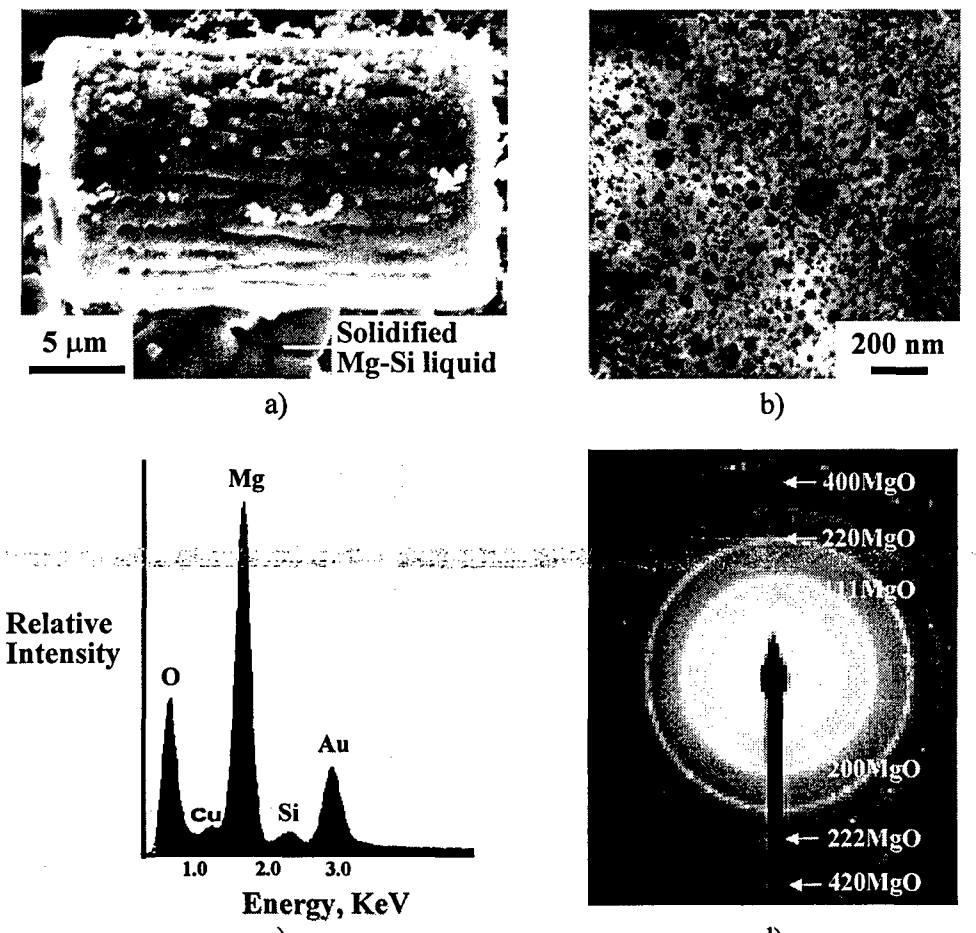

Fig. 2. a) Secondary electron image of an *Aulacoseira* frustule after exposure to Mg(g) for 0.5 h at 700°C. b) Transmission electron microscope image, c) EDX analysis, and d) electron diffraction analysis of an electron transparent cross-section of an *Aulacoseira* frustule after exposure to Mg(g) for 0.5 h at 700°C.

liquid (a eutectic liquid can form at 638°C in the Mg-Si system) that poured out of the frustule. The solidified Mg-Si liquid can be seen below the MgO-converted frustule in Fig. 2a. The data in Fig. 2 indicate that *Aulacoseira* frustules can be fully converted into a nanocrystalline MgO-based replica within only 0.5 h of exposure to Mg(g) at 700°C.

In order to evaluate the phase and nanostructural evolution during such shape-preserving reactive conversion, the reaction temperature was further reduced to 650°C to slow the rate of reaction. XRD analyses of the *Aulacoseira* diatom frustules before and after exposure to Mg(g) for various times at 650°C are shown in Fig. 3. For exposure times of 1 h or less, only diffraction peaks for SiO_2 (as cristobalite) were detected. However, from 1.5 to 2 h of exposure to Mg(g), MgO, Si and Mg_2Si formed at the expense of cristobalite. Indeed, after the 2 h treatment, the diffraction peaks for cristobalite vanished. Bright field TEM images, and associated electron diffraction patterns, of ion-milled cross-sections obtained from specimens exposed to Mg(g) for 1-2 h at 650°C are shown in Figs. 4a-f. Consistent with XRD analyses, selected area electron diffraction (SAED) analyses of the cross-section of the 1 h specimen in Fig. 4a revealed only diffraction associated with cristobalite (hkl values associated with

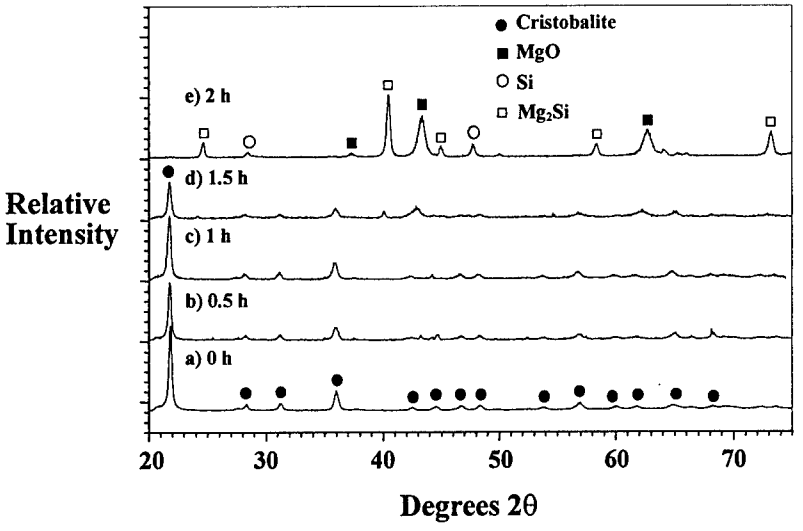

Fig. 3. XRD analyses of *Aulacoseira* diatom frustules a) before and b)-e) after exposure to magnesium gas at 650°C for 0.5, 1, 1.5 and 2 h.

several of these diffraction spots are indicated). Prolonged exposure of this specimen cross-section to the electron beam in the TEM also resulted in amorphization, as has been observed by other authors during TEM analyses of silica-based specimens. After 1.5 h of reaction, the specimen cross-section was found to be partially reacted (Fig. 4b). SAED analysis of the reaction zone (Fig. 4e) revealed the presence of MgO and Si, consistent with reaction (1). The absence of electron or x-ray diffraction peaks (Figs. 3d and 4e) for magnesium silicates (e.g., forsterite, Mg_2SiO_4; enstatite, $MgSiO_4$) suggested that these compounds were not involved as intermediate products in reaction (1). Consistent with such diffraction analyses, a high-resolution TEM image (Fig. 5) of this cross-section obtained at the location of the interface between the reacted zone and the unreacted silica revealed the presence of only MgO and Si nanocrystals ($\leq$ 5 nm in diameter) in an amorphous matrix. The structure generated after 2 h of exposure to Mg(g) at 650°C is shown in Fig. 4c. The nanocrystalline reaction zone completely penetrated this specimen. SAED analysis revealed a mixture of MgO, Si, and Mg_2Si in the

reaction zone. The latter compound was generated by the continued reaction of the silicon product from reaction (1) with magnesium gas, as shown below.

$$2Mg(g) + Si(s) \Rightarrow Mg_2Si(s) \qquad (5)$$

As discussed above, further reaction of this Mg_2Si product with Mg(g) leads to the formation of a Mg-Si liquid that tends to pour out of the converted frustule onto the underlying steel substrate (Fig. 2a), so as to leave a nanocrystalline MgO-based structure. The width of the most intense x-ray diffraction peak for magnesia (the (200) peak near 2θ = 43 degrees) was obtained from several batches of specimens exposed to the 650°C/2 h heat treatment. Insertion of this data into the Scherrer equation yielded average magnesia crystallite sizes of 12-15 nm. These XRD-derived values were consistent with the fine nanocrystallites observed in the TEM images of Figs. 4b and c. These MgO grains were also considerably finer, by several orders of magnitude, than those generated upon exposure of diatom silica to magnesium gas at 900°C for 4 h.

Prior work by other authors on the reaction of sintered SiO_2(s) tablets or quartz crystals with Mg(g) at much higher temperatures (e.g., 1150°C) have indicated that Mg_2SiO_4(s) and SiO(g)

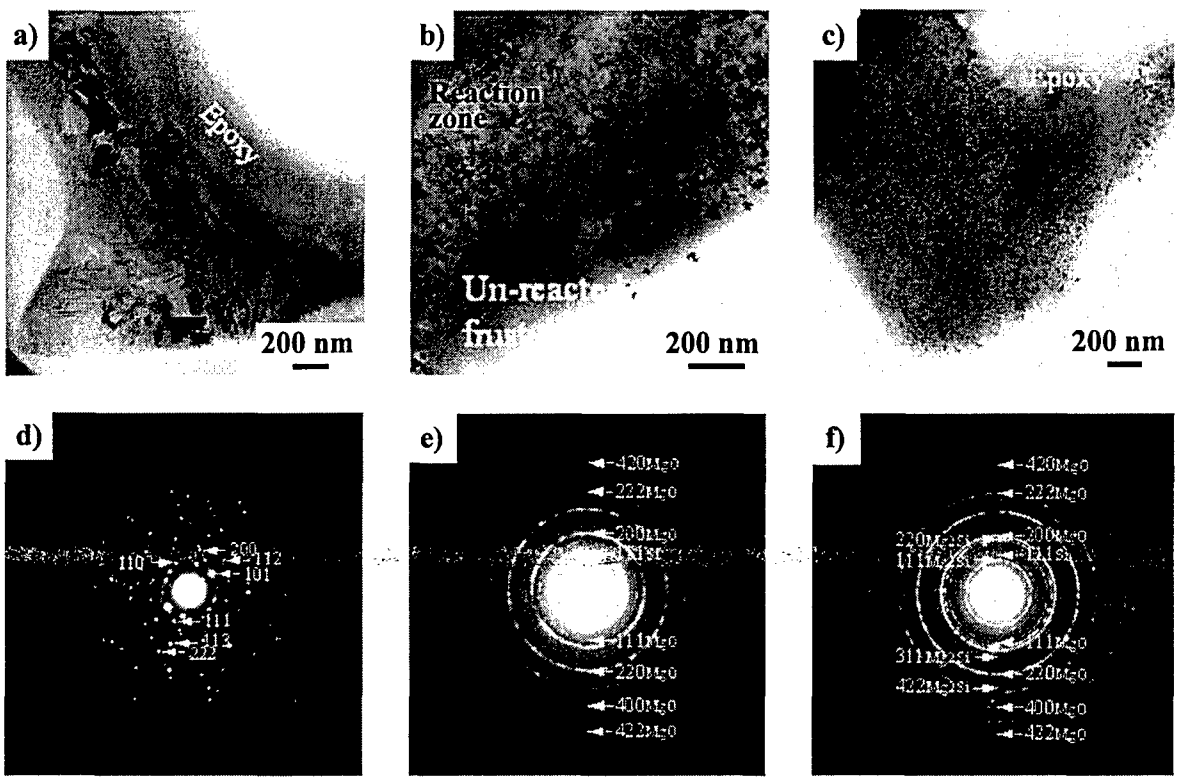

Fig. 4. a)-c) TEM images of cross-sections of *Aulacoseira* frustules exposed to Mg gas at 650°C for 1, 1.5, and 2 h respectively. d)-f) SAED patterns obtained from a)-c) respectively.

formed as intermediate reaction products via the following reaction steps:

$$3SiO_2(s) + 2Mg(g) \Rightarrow Mg_2SiO_4(s) + 2SiO(g) \qquad (6)$$

$$Mg_2SiO_4(s) + 2Mg(g) \Rightarrow 4MgO(s) + Si(s) \qquad (7)$$

$$2SiO(g) + 2Mg(g) \Rightarrow 2MgO(s) + 2Si(s) \qquad (8)$$

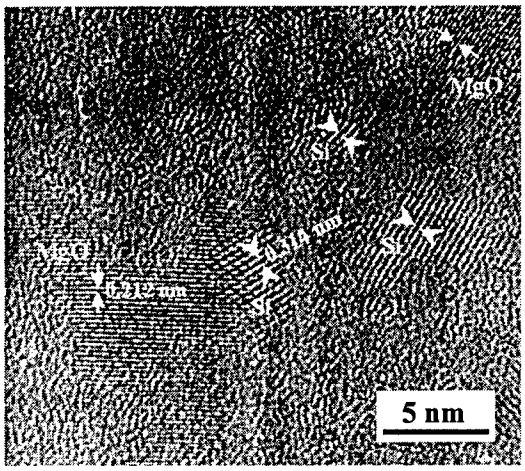

Fig. 5. High-resolution TEM image of a cross-section of an *Aulacoseira* diatom frustule exposed to Mg gas at 650°C for 1.5 h (obtained at the reaction front seen in Fig. 4b).

While the formation of Mg_2SiO_4(s) and SiO(g) via reaction (6) was thermodynamically favored at 1150°C, this reaction was not favored at 650°C in the present work. The thermodynamic ratio of the Mg(g) to SiO(g) partial pressures that is required for reaction (6) to proceed spontaneously to the right at 650°C is 48, compared to only $6.5X10^{-2}$ at 1150°C. The amount of Mg relative to SiO_2 that was sealed in the steel ampoules in the present work (a molar Mg:SiO_2 ratio of 9.9:1) was insufficient to allow for the occurrence of this intermediate reaction.

The basic understanding of the phase and nanostructural evolution obtained from the work discussed above has enabled the development of optimized processing treatments over the past year for the conversion of SiO_2 frustules into MgO-based frustules containing minimal secondary phases (i.e., Si or Mg_2Si). By minimizing these secondary phases, the MgO frustules could be utilized as chemically-compatible substrates for other functional ceramic coatings (e.g., luminescent Eu-doped $BaTiO_3$) and as structures for microfluidic mixing devices (e.g., based on electroosmotic flow). Optimization of the MgO conversion conditions is discussed below.

Optimized Processing of MgO-converted Frustules

Several processing changes have been introduced in order to reduce the relative amounts of undesired second phases (e.g., Si, Mg_2Si) in the MgO-converted frustules. A schematic of a typical reaction configuration within the sealed iron tubes is shown in Fig. 6a. At the start of the experiments, the diatom frustules and solid magnesium reactants were placed at opposite ends of the iron tube. The tube was then crimped in the middle (to avoid physical mixing of the reactants) and the ends were welded shut. Upon heating the magnesium vaporized and diffused to the frustules, whereupon the displacement reaction commenced. As shown in Figs. 6a and 6b, distinct reaction zones were detected within partially-converted frustule powder beds. The distinct interfaces and colors of these zones enabled separation and analyses (XRD, SEM, EDX) of the phases within each zone. The region located nearest the magnesium gas source was observed to possess a grey or blue-grey color, which was a result of the presence of Mg_2Si. A secondary electron image of this phase is shown in Fig. 6c. The darker intermediate zone was comprised of a mixture of MgO and Si. A secondary electron image of a frustule from within this zone, exhibiting Si nodules, is shown in Fig. 6d. The brown zone at the opposite end of the

powder bed contained residual unreacted silica. The distribution of these products was consistent with the reaction steps identified above; that is, SiO_2 is first converted into a mixture of MgO and Si, and the Si then reacts with excess Mg(g) to form Mg_2Si.

The $Mg:SiO_2$ reactant ratio, the reaction temperature, and the reaction time were varied to allow for complete conversion of the SiO_2 into MgO while minimizing the amount of Mg_2Si produced. With a $Mg:SiO_2$ ratio of 2:1 and a reaction temperature/time of 900°C/1.5 h, the frustule powder bed was converted into a mixture of MgO and Si with minimal Mg_2Si, as shown in Fig. 7a. The residual silicon was then selectively dissolved away with an aqueous sodium hydroxide solution. The NaOH in this solution was adjusted to achieve a NaOH:Si molar ratio of 2:1 to allow for the formation of soluble sodium metasilicate (Na_2SiO_3). The Si-depleted frustules were then rinsed with boiling DI water. XRD analysis and secondary electron images of the resulting MgO frustules are shown in Figs. 7b and 8, respectively. It is important to note that the development of processing methods for removing Mg_2Si (through adjustment of reaction conditions) and Si (through selective dissolution) were essential for the use of MgO frustules as: i) substrates for conformal luminescent coatings (i.e., Eu-doped $BaTiO_3$ coatings on MgO), and ii) 3-D micro-structures for incorporation in electro-osmotic mixing devices (i.e., to avoid bubble formation due to the reaction of residual Mg_2Si with water).

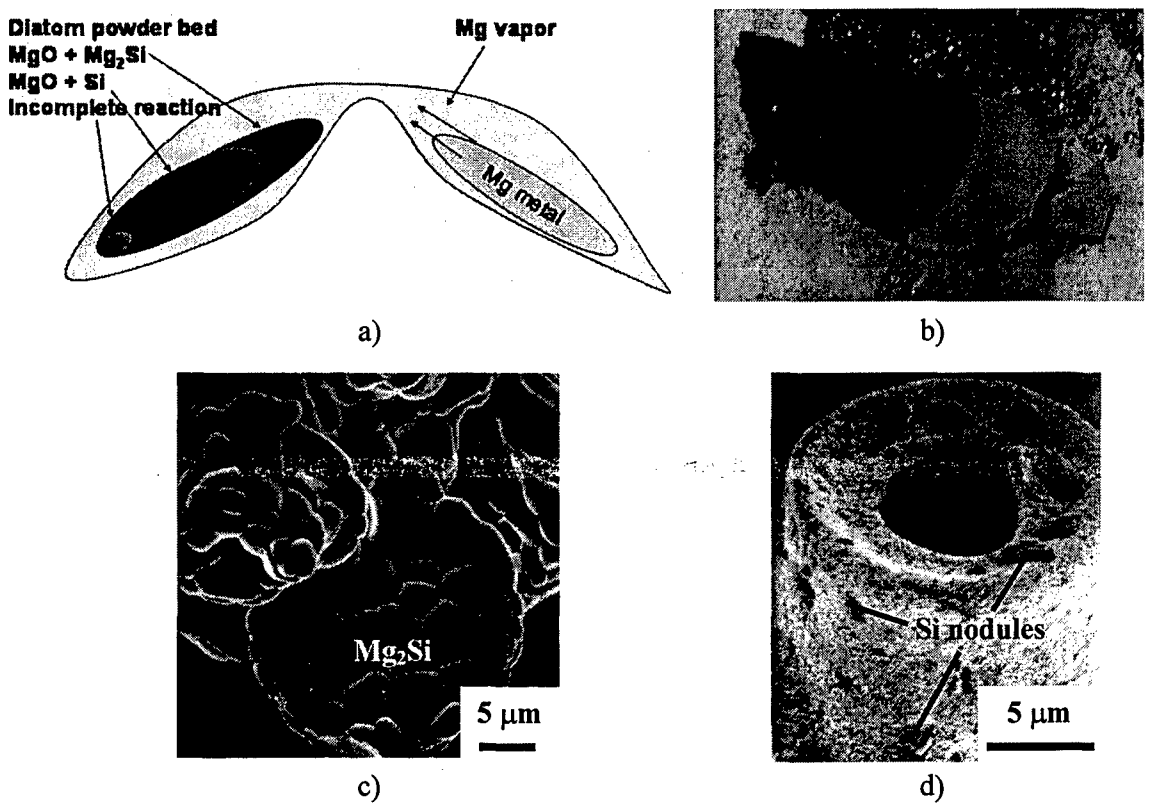

Fig. 6. a) Schematic illustration of the sealed iron reaction tube showing the positioning of reactants and the typical progression of products through the frustule powder bed. b) Optical image of a frustule powder bed after reaction for 3 h at 850°C. Secondary electron images revealing the Mg_2Si and Si secondary phases are shown in c) and d), respectively.

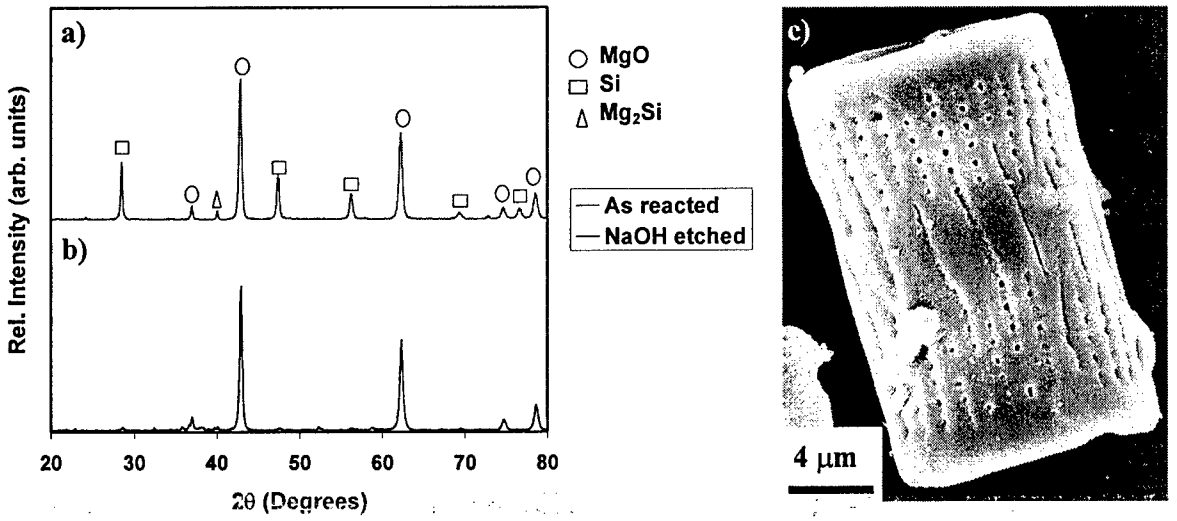

Fig. 7. XRD analyses of MgO-converted diatoms a) before and b) after selective silicon dissolution with an aqueous sodium hydroxide solution. c) Secondary electron image of the MgO frustule corresponding to the XRD pattern in b).

Reactive Conversion into TiO_2 (anatase) Frustules

A two-step reaction process has been used to convert silica-based diatom frustules into titania replicas. The first step involves the following metathetic reaction of SiO_2 with $TiF_4(g)$ to yield the oxyfluoride, $TiOF_2$:

$$2TiF_4(g) + SiO_2(s) \Rightarrow 2TiOF_2(s) + SiF_4(g) \qquad (9)$$

In the second step, the $TiOF_2$ is converted to TiO_2 by reaction with $O_2(g)$:

$$TiOF_2(s) + O_2(s) \Rightarrow TiO_2(s) + F_2(g) \qquad (10)$$

In this work, solid TiF_4 was utilized as a low-temperature source of TiF_4 vapor (note: the sublimation temperature of $TiF_4(s)$ is 285°C). 100 milligrams of *Aulacoseira* diatom frustules were placed within a titanium tube along with solid TiF_4. As discussed above for the Mg/SiO_2 reactions, both ends of the tube were then crimped and welded shut. The specimen-bearing tube was then heated to the desired reaction temperature. At the end of this treatment, the tube was pushed out of the hot zone of the horizontal tube furnace. For the second reaction, the specimens were heated to 350°C for 2 h in pure, flowing oxygen.

Several processing parameters associated with the first reaction step have been found to be particularly critical with regards to shape preservation:

i) the $TiF_4:SiO_2$ reactant ratio
ii) the peak reaction temperature and time
iii) the heating rate

Initial experiments conducted at 500-700°C for 2 h using $TiF_4:SiO_2$ molar ratios of $\geq$4.9:1 within the sealed Ti tubes resulted in disintegration of the starting SiO_2 frustules and the formation of relatively coarse plate-shaped TiO_2 crystals (5-10 μm X 5-10 μm X 0.5-1 μm thick). Such active vaporization of the silica frustules was avoided by lowering the reaction temperature to 350°C and reducing the $TiF_4:SiO_2$ molar ratio to 2.4:1 within the Ti tubes. After 2 h under these conditions, the overall shape and fine features of the reacted frustule were quite similar to those

of the starting frustules, as shown in Fig. 8a below. EDX and XRD analyses confirmed that the frustules had been converted completely into $TiOF_2$. Further reduction in the TiF_4:SiO_2 molar ratio to 1.6 resulted in negligible reaction of the frustules within 2 h at 350°C.

An increase in the reaction temperature from 350°C to 450°C for a fixed time (2 h), a fixed heating rate (5°C/min), and a fixed TiF_4:SiO_2 ratio resulted in appreciable coarsening of the $TiOF_2$ grains, as shown in Figs. 8a and 8b. For a constant peak temperature/time of 350°C/2 h, a reduction in the heating rate also yielded an increase in $TiOF_2$ crystallite size (Figs. 8c and 8d). At such modest temperatures and times, it is not likely that such coarsening occurred by a solid-state diffusion mechanism. Given that a gaseous $TiOF_2$ species can exist at these temperatures, it is likely that such rapid coarsening occurred via transport through the gas phase; that is, by the evaporation of small $TiOF_2$ particles and condensation onto larger $TiOF_2$ particles (Ostwald ripening) as illustrated in Fig. 8e. Such gas-phase-assisted coarsening has been observed in a number of ceramic systems with volatile species (notably by D. W. Readey: "Vapor Transport and Microstructure Development in Ceramics," Journal of Metals, **36** (12) 18-18, 1984).

By controlling the heating rate, peak reaction temperature and time, and TiF_4:SiO_2 molar ratio, the active vaporization of silica and the rapid vapor-phase-assisted coarsening of $TiOF_2$ could be minimized so as to yield $TiOF_2$ and then TiO_2 replicas that retained the shapes and fine features of the starting diatom frustules.

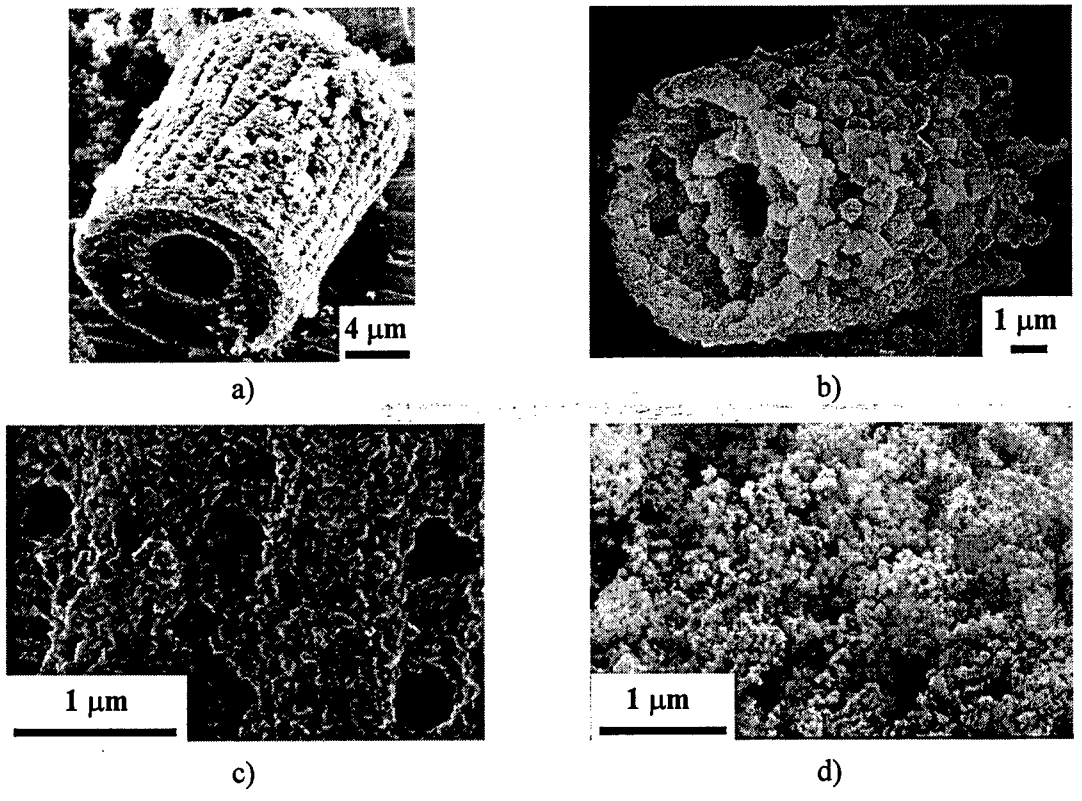

Fig. 8. Secondary electron images of $TiOF_2$-converted frustules generated by reaction for 2 h at: a) 350°C (heating rate = 5°C/min), b) 450°C (heating rate = 5°C/min). Higher magnification images of $TiOF_2$-converted frustules after reaction for 2 h at 350°C with heating: c) at a rate of 5°C/min and d) via thrusting into pre-heated furnace.

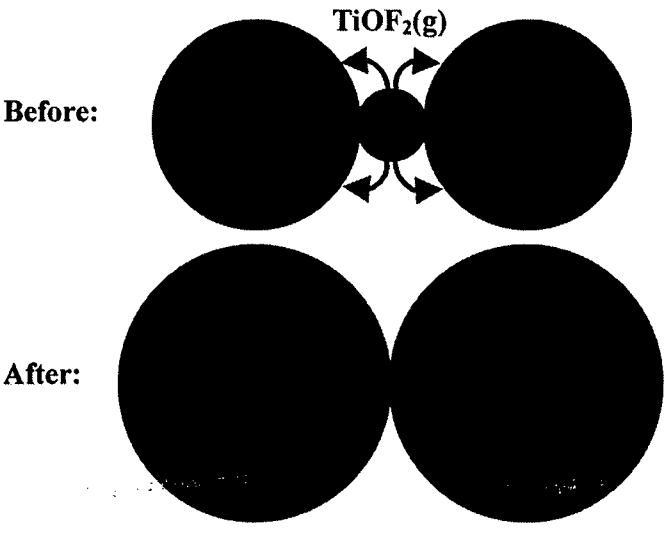

e)

Fig. 8 (cont.). A schematic illustrating gas-phase-assisted coarsening is shown in e).

Reactive Conversion into ZrO_2 Frustules

The direct reaction of $ZrF_4(g)$ with SiO_2 diatom frustules was conducted within sealed nickel alloy tubes for 2 h over a range of temperatures (250-800°C) and ZrF_4:SiO_2 molar ratios (0.36 to 3.6). For reaction temperatures at or below 350°C, no reaction was detected within 2 h. At higher temperatures and for all ZrF_4:SiO_2 ratios examined, the silica frustules were observed to disintegrate, as shown in Fig. 9.

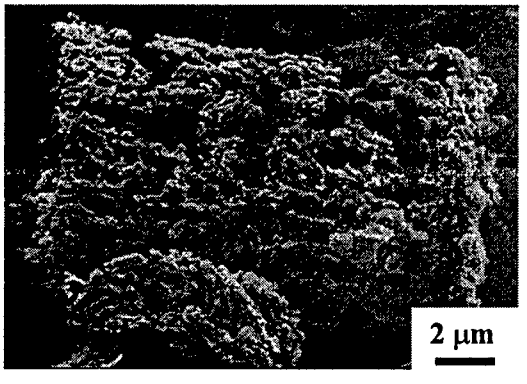

Fig. 9. Secondary electron image of a disintegrating *Aulacoseira* frustule after exposure to ZrF_4 gas at 600°C for 2 h.

An entirely different two-step reaction process was then adopted so as to avoid such active vaporization. In the first step, the silica frustules were converted into MgO, as per the oxidation-reduction conditions discussed above. The magnesia was then exposed to $ZrCl_4(g)$ to allow for the following net reaction:

$$ZrCl_4(g) + MgO(s) \Rightarrow ZrO_2(s) + MgCl_2(l) \qquad (11)$$

The magnesium chloride product, which solidified upon cooling to room temperature, was then be removed by selective dissolution in water. To test this new approach, the magnesia-converted frustules were sealed along with zirconium chloride ($ZrCl_4$:MgO molar ratio = 5.8) in nickel alloy tubes. The tubes were then heated at 5°C/min to a peak temperature of 325-650°C for 2 h. The reacted specimens were then immersed and stirred in water heated to 80°C for 1 h. For reaction temperatures at or below 475°C, significant amounts of residual unreacted magnesium oxide were detected. However, reaction for 2 h at 650°C resulted in complete conversion of the magnesia into tetragonal zirconia and magnesium chloride. An XRD pattern of such reacted specimens (after dissolution of the magnesium chloride in water) is shown in Fig. 10. Secondary electron images of zirconia-converted frustules and a corresponding EDX pattern are shown in Figs. 11a-c. The zirconia replica retained the cylindrical shape of the starting *Aulacoseira* frustule.

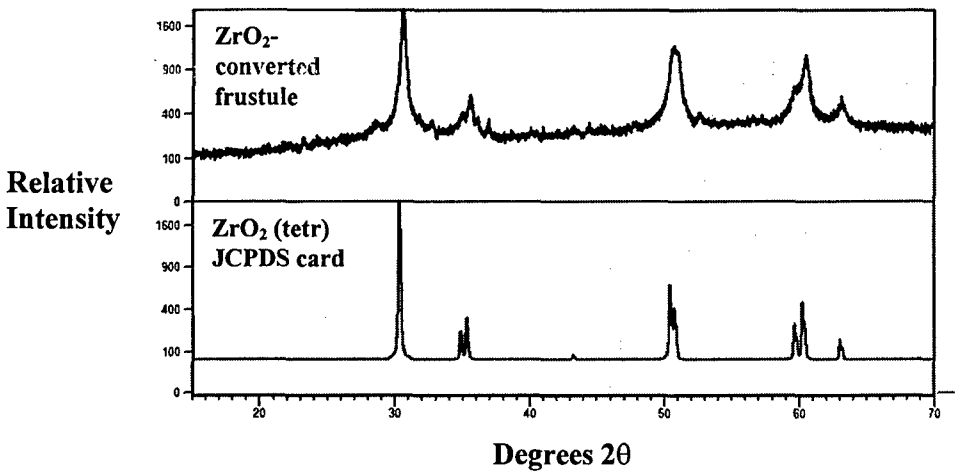

Fig. 10. XRD pattern obtained from a ZrO_2-converted frustule generated by exposure of a MgO-converted frustule to $ZrCl_4$(g) for 2 h at 650°C followed by immersion in stirred water at 80°C for 1 h.

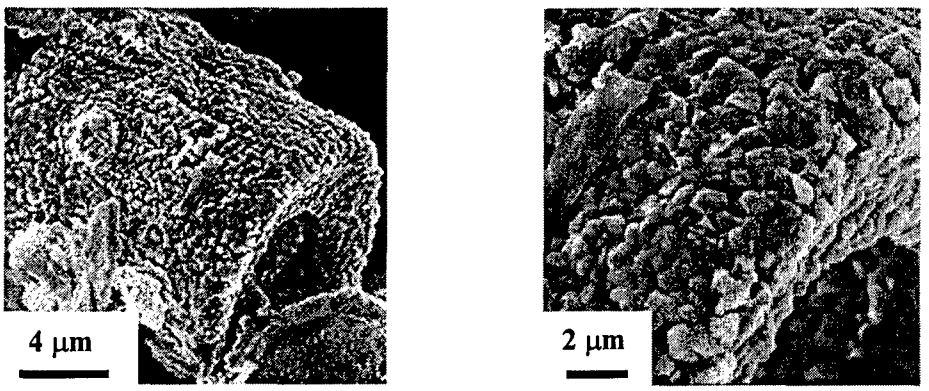

a) b)

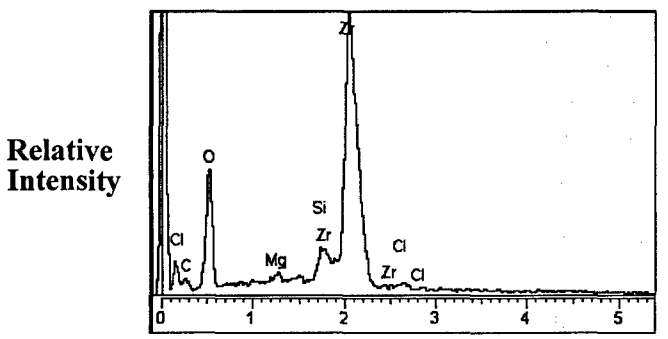

c)

Fig. 11. a), b) Secondary electron images, and c) an associated EDX pattern obtained from a ZrO_2-converted frustule generated by exposure of a MgO-converted frustule to $ZrCl_4(g)$ for 2 h at 650°C followed by immersion in stirred water at 80°C for 1 h.

Personnel Supported:

Faculty:	Prof. Ken H. Sandhage
Graduate Students:	Mr. Samuel Shian
	Mr. Shawn Allan
	Mr. Matthew Dickerson

Publications:

1. Y. Cai*, S. M. Allan, F. M. Zalar, K. H. Sandhage, "Three-dimensional Magnesia-based Nanocrystal Assemblies via Low-Temperature Magnesiothermic Reaction of Diatom Microshells," J. Am. Ceram. Soc., **88** [7] 2005-2010 (2005).
2. M. B. Dickerson, R. R. Naik, P. M Sarosi, G. Agarwal, M. O. Stone, K. H. Sandhage, "Ceramic Nanoparticle Assemblies with Tailored Shapes and Tailored Chemistries via Biosculpting and Shape-preserving Inorganic Conversion," J. Nanosci. Nanotech., **5** [1] 63-67 (2005).
3. M. R. Weatherspoon*, S. M. Allan, E. Hunt*, Y. Cai*, K. H. Sandhage, "Sol-Gel Synthesis on Self-Replicating Single-Cell Scaffolds: Applying Complex Chemistries to Nature's 3-D Nanostructured Templates," Chem. Comm., [5] 651-653 (2005).
4. M. B. Dickerson, R. R. Naik, M. O. Stone, Y. Cai*, and K. H. Sandhage, "Identification of Peptides that Promote the Rapid Precipitation of Germania Nanoparticle Networks via Use of a Peptide Display Library," Chem. Comm., **15**, 1776-1777 (2004).
5. R. R. Unocic, F. M. Zalar, Peter M. Sarosi, Ye Cai*, and K. H. Sandhage, "Anatase Assemblies from Algae: Coupling Biological Self-assembly of 3-D Nanoparticle Structures with Synthetic Reaction Chemistry," Chem. Comm., [7] 795-796 (2004).

*supported by an AFOSR MURI project.

Interactions/Transitions:

The Sandhage group has moved from Ohio State University to the Georgia Institute of Technology. New facilities that have been set up at Georgia Tech for the Sandhage group over the past year include:

- a diatom culturing facility (with the advice and help of M. Hildebrand, UCSD/Scripps)
- a biopanning facility (with the advice and help of R. Naik, AFRL)
- new thermal processing facilities (with the advice and help of R. Rapp, Ohio State)

A new state-of-the-art x-ray characterization facility (which includes a high-temperature x-ray diffraction system for the work in this BIC program) has also been established over the past year by R. Snyder, a collaborator with K. Sandhage.

The reaction-based processes developed in this BioInspired Concepts (BIC) project have enabled the syntheses of frustule-shaped structures (via a MURI project) that exhibit:

i) luminescence (from Eu/$BaTiO_3$ coatings applied to compatible MgO-converted frustules)

ii) gas sensing (due to rapid changes in the conductivity of TiO_2 frustules resulting from small changes in ethanol vapor pressure)

iii) organophosphor destruction (pesticide-bearing solutions have exhibited rapid reaction with TiO_2-converted frustules)

Luminescence measurements have been obtained via a new collaboration with Prof. Chris Summers of the MSE Dept. at Georgia Tech. Gas sensing measurements have been obtained via a new collaboration with Prof. Meilin Liu of the MSE Dept. at Georgia Tech. Organophosphor destruction kinetics have been measured in a new collaboration with Prof. Ching-Hua Huang of the Civil and Environmental Engineering Dept. at Georgia Tech.

Other interactions include the following technical presentations:

1. M. S. Haluska, K. H. Sandhage, R. L. Snyder, S. T. Misture, "High Temperature In-Situ X-ray Diffraction of the Mg(g)/SiO_2(s) Diatom Displacement Reaction," 53rd Annual Denver X-ray Conference, Denver, CO, August 3, 2004.
2. R. L. Snyder, K. H. Sandhage, "A Novel Biology-based Route to Three-Dimensional Nanoparticle Assemblies with Intricate Shapes, Nanoscale Features, and Tailored Chemistries: Bioclastic and Shape-preserving Inorganic Conversion (BaSIC)," Plenary talk, 7th International Workshop on High-Temperature Superconductors and Novel Inorganic Materials Engineering, Moscow, Russia, June 20-25, 2004.
3. K. H. Sandhage, C. Gaddis, M. Dickerson, S. Allan, P. Graham, S. Shian, M. Weatherspoon, Y. Cai, R. R. Naik, M. O. Stone, "A Hybrid (Biogenic/Synthetic) Route to 3-D Nanoparticle Assemblies with Tailored Chemistries: the Bioclastic and Shape-preserving Inorganic Conversion (BaSIC) Process," Invited talk, MRS Spring Meeting, San Francisco, CA, March 12-16, 2004.
4. S. Allan, M. Dickerson, C. Gaddis, S. Shian, R. R. Unocic, F. M. Zalar, Y. Cai, E. Hunt, K. H. Sandhage, R. R. Naik, M. O. Stone, M. Hildebrand, B.P. Palenik, "3-D Nanoparticle Structures with Self-Replicating Shapes and Synthetically-Tailored Compositions," 133rd Annual TMS Meeting, Charlotte, NC, March 16, 2004.
5. K. H. Sandhage, C. S. Gaddis, M. B. Dickerson, S. Shian, R. R. Naik, M. O. Stone, M. M. Hildebrand, B. P. Palenik, "The BaSIC Route to 3-D Nanoparticle Assemblies with Self-Replicating, Genetically-Tailored Shapes and Synthetically-Tailored Chemistries," 28th International Cocoa Beach Conf. and Exposition on Advanced Ceramics and Composites, Cocoa Beach, FL, January 27, 2004.
6. C. S. Gaddis, J. Zhao, K. H. Sandhage, "A Transient Bioscaffolding Route to Chemically-Tailored, Nanoparticle-based Assemblies with Complex 3-D Shapes and Fine (Meso-to-Nanoscale) Features," Materials Research Society Fall Meeting, Boston, MA, December 2, 2003.
7. R. R. Unocic, F. M. Zalar, K. H. Sandhage, "A Hybrid (Biogenic/Synthetic) Route to 3-D Nanoparticle Assemblies with Tailored Chemistries: The Bioclastic and Shape-preserving Inorganic Conversion (BaSIC) Process," Materials Research Society Fall Meeting, Boston, MA, December 2, 2003.
6. K. H. Sandhage, M. B. Dickerson, P. M. Sarosi, G. Agarwal, R. R. Naik, M. O. Stone, "Chemical Transformation of Diatoms," Invited talk, Diatom Nanotechnology Workshop at the North American Diatom Society meeting, Florida Keys, October 22-26, 2003.
7. K. H. Sandhage, "Chemically-Tailored 3-D Nanoparticle Structures by the BaSIC (Bioclastic and Shape-preserving Inorganic Conversion) Process," Invited talk, Composites at Lake Louise Conference, Lake Louise, Canada, October 21, 2003.